

# Multiple-Color Electrochromism from Layer-by-Layer-Assembled Polyaniline/Prussian Blue Nanocomposite Thin Films

Dean M. DeLongchamp<sup>†</sup> and Paula T. Hammond\*

Department of Chemical Engineering, Massachusetts Institute of Technology,  
Cambridge, Massachusetts 02139-4307

Received March 1, 2004. Revised Manuscript Received July 7, 2004

The creation of new materials systems for lightweight and flexible displays is an extremely active research field. Electrochromic displays possess a keen advantage over other technologies because it is possible for a single electrochromic pixel to produce multiple colors in addition to white, depending on applied potential. This possibility has proven quite challenging to achieve in practice. Here we present the successful fabrication of a multiply colored electrochromic electrode using layer-by-layer (LBL) assembly. The electrode films are created by exploiting intrinsic electrostatic attraction between the polycation poly(aniline) (PANI) and a negatively ionized Prussian Blue (PB) nanoparticle dispersion. The resultant organic/inorganic nanocomposites exhibit excellent smoothness and a classical linear increase in film thickness with assembly exposure steps. Electrochemical and spectrophotometric characterization confirms the distinct and noninteracting contributions from PANI and PB and reveals that both are fully electrochemically accessible even in thick, high contrast films. Switching speed is accelerated due to the incorporation of electronically conducting PANI. The PANI/PB nanocomposite undergoes an uncolored to green to blue transition over the potential range from  $-0.2$  to  $0.6$  V vs K-SCE. These results validate an LBL-assembly-based intermixing strategy for the design of multiple-hue electrochromic electrode films. Future horizons include extension to other materials, with the eventual goal of creating a single electrode film or electrochemical cell capable of displaying any visible color on demand.

## Introduction

Intense speculation exists in academic and industrial circles concerning the potential emergence of a single dominant next-generation display technology to replace cathode ray tubes and liquid crystal displays. Once the dust settles, it is likely that several niche technologies will have developed to provide tailored performance, cost, and form factor to a targeted user and environment. In many circumstances consumers may desire a paperlike reading experience in a dynamic format. Two technologies have arisen to meet the demand for a flexible, reflective display: electrodynamics and electrochromics. Electrodynamics displays rely on electrophoretic migration or rotation of pigmented particles within a flexible laminate to create an image.<sup>1–3</sup> These mechanisms can achieve high contrast, but switching speed is limited by particle dynamics, and multiple colors must be introduced by pigmentation and patterning particles or by employing a contrast-lowering color filter. Electrochromic displays exploit redox-active materials with multiple stable valence states featuring different

intrinsic colorations.<sup>4–6</sup> The electrochromic materials chosen for modern displays are often polymers, because they are capable of facile synthetic variation, straightforward device integration, and mechanical flexibility.<sup>7–10</sup> Electrochemical alteration of the valence state of an electrochromic polymer brings about a concomitant change in its reflected or transmitted visible spectrum. Recent commercialization of electrochromic elements has been assisted by the enhancement of switching speed and contrast that can be achieved by employing mesoporous electrodes that reduce ion diffusion distances and enhance absorbance by multiple scattering events.<sup>11,12</sup>

(4) Monk, P. M. S.; Mortimer, R. J.; Rosseinsky, D. R. *Electrochromism: Fundamentals and Applications*; Weinheim: New York, 1995.

(5) Mortimer, R. J. *Chem. Soc. Rev.* **1997**, 26, 147.

(6) Somani, P. R.; Radhakrishnan, S. *Mater. Chem. Phys.* **2003**, 77, 117.

(7) Boehme, J. L.; Mudigonda, D. S. K.; Ferraris, J. P. *Chem. Mater.* **2001**, 13, 4469.

(8) Meeker, D. L.; Mudigonda, D. S. K.; Osborn, J. M.; Loveday, D. C.; Ferraris, J. P. *Macromolecules* **1998**, 31, 2943.

(9) Thompson, B. C.; Schottland, P.; Zong, K.; Reynolds, J. R. *Chem. Mater.* **2000**, 12, 1563.

(10) Argun, A. A.; Cirpan, A.; Reynolds, J. R. *Adv. Mater.* **2003**, 15, 1338.

(11) Bach, U.; Corr, D.; Lupo, D.; Pichot, F.; Ryan, M. *Adv. Mater.* **2002**, 14, 845.

(12) Corr, D.; Bach, U.; Fay, D.; Kinsella, M.; McAtamney, C.; O'Reilly, F.; Rao, S. N.; Stobie, N. *Solid State Ion.* **2003**, 165, 315.

\* Corresponding author. E-mail: hammond@mit.edu.

<sup>†</sup> Current address: National Institute of Standards and Technology, Polymers Division, Gaithersburg, Maryland.

(1) Sheridan, N. K.; Berkovitz, M. A. *Proc. Soc.* **1977**, 18, 289.

(2) Comiskey, B.; Albert, J. D.; Yoshizawa, H.; Jacobson, J. *Nature* **1998**, 394, 253.

(3) Lean, R. C. *J. Imaging Sci. Technol.* **2002**, 46, 562.

A primary advantage that electrochromics hold over electrodynamic displays is that a single electrochromic electrode can in theory display different colors at different applied potentials. If this advantage were fully exploited so that a single film could be made to reflect any point within a cyan–magenta–yellow–black (CMYK) color space, the fabrication of a flexible, lightweight, and full-color display laminate would be greatly simplified. Because single electrochromic materials can rarely achieve more than two differently colored, stable oxidation states without the use of expensive materials<sup>13,14</sup> or complex syntheses,<sup>15</sup> multiply colored electrochromic films may be created in the near term by combining two or more electrochromic materials into a single electrode film.

Perhaps the most ideal method to combine two materials in such a fashion is the layer-by-layer (LBL) assembly technique. In LBL assembly, a thin film is grown up from a substrate by alternating its exposure to aqueous solutions containing species with opposite multivalent attractive affinities.<sup>16–19</sup> Upon each exposure, one component deposits to overcompensate the surface affinity, causing reversal of that affinity and allowing the deposition of a layer of opposite affinity. The most commonly employed LBL assembly interactions are electrostatic, where a film is created by combining a polycation and a polyanion.<sup>20</sup> Films created by LBL assembly are inherently two-component composites and can be designed to provide practically any type of functional performance. This technique has been employed to create high-quality electrochromic electrode films.<sup>21–28</sup> Full exploitation of the technique by the combination of two similarly coloring electrochromic materials has resulted in electrode films possessing extremely high contrast.<sup>26</sup>

It is the objective of this work to create a multiply colored electrochromic electrode by combining two differently coloring electrochromic materials into the same film using LBL assembly. Multihued states are attained by combining the polycation poly(aniline) (PANI) and an anionic nanoparticle dispersion of iron(III) hexacyanoferrate(II) (Prussian Blue, PB). PANI changes from

a colorless reduced state (leucoemeraldine salt) to a green/blue oxidized state (emeraldine salt). The color of PB nanocrystals changes from a colorless reduced state (Prussian White, PW), to a deep cyan oxidized state. Both of these transitions occur over the same potential range:  $-0.2$  to  $0.6$  V. Importantly, PANI passes through a yellow intermediate state while the PB passes through a pale blue intermediate state. By the additive pigment palette, the PANI/PB composite should be nearly colorless at  $-0.2$  V, pass through a green intermediate state, and finally become blue at  $0.6$  V. Although green and blue colors are not proper axes to span a CMYK color space, we present this work as a proof of concept.

Combining the electrochromic capabilities of PANI and PB is an attractive goal and has been explored previously using electrochemically deposited films. Some of these investigations employed PANI and PB within the same electrode.<sup>29–32</sup> Others employed PANI and PB as opposing cathode and anode (respectively) during coloration in a low-contrast green-to-blue electrochromic cell scheme; this two-color cell exhibited no uncolored state.<sup>33,34</sup> In one notable study, Jelle and Hagen determined that the simultaneous or “intermixed” electrochemical deposition of PANI and PB onto a single electrode resulted in superior coloration and stability over a PANI + PB bilayer electrode,<sup>35</sup> a result that provides impetus for the application of the LBL method, which provides fine control over such intermixing. Thus far there have been no published efforts to combine these two materials in a self-assembled composite. Working from our recent successful incorporation of PB into a LBL assembled film with linear poly(ethylene imine) (LPEI),<sup>28</sup> we now combine PB with the conjugated electrochromic polymer PANI. This strategy possesses an advantage over electrochemical deposition because the PANI chemistry and PB crystal size can be precisely controlled. The formation of nanometer-scale PB crystals in solution, thereafter combined in a LBL assembled film with a polyelectrolyte, results in a faster switching and higher contrast electrode film than can be prepared by electrochemical means.<sup>28</sup> Herein we present the assembly, electrochemical characterization, and spectroelectrochemistry of PANI/PB nanocomposites. A primary result is the realization of multicolor electrochromism from LBL blending. Facile extension to other materials could provide multiply colored electrochromic films to support full-color displays or cheap and flexible color-adaptive raiment.

## Experimental Section

**Materials.** The PANI (Aldrich) solution was  $0.01$  M with respect to the repeat unit molecular weight, prepared using a 1:9 dimethylacetamide and water solvent pair as described by

- (13) Liu, Y. Q.; Shigehara, K.; Yamada, A. *Thin Solid Films* **1989**, *179*, 303.
- (14) Rodriguezmendez, M. L.; Aroca, R.; Desaja, J. A. *Chem. Mater.* **1993**, *5*, 933.
- (15) Sotzing, G. A.; Reddinger, J. L.; Katritzky, A. R.; Soloduch, J.; Musgrave, R.; Reynolds, J. R. *Chem. Mater.* **1997**, *9*, 1578.
- (16) Decher, G. *Science* **1997**, *277*, 1232.
- (17) Hammond, P. T. *Curr. Opin. Colloid Interface Sci.* **2000**, *4*, 430.
- (18) Decher, G.; Schlenoff, J. B.; Eds. *Multilayer thin films*; Wiley: Weinheim, 2003.
- (19) Schonhoff, M. *Curr. Opin. Colloid Interface Sci.* **2003**, *8*, 86.
- (20) Decher, G.; Hong, J. D.; Schmitt, J. *Thin Solid Films* **1992**, *210*, 831.
- (21) Stepp, J.; Schlenoff, J. B. *J. Electrochem. Soc.* **1997**, *144*, L155.
- (22) Schlenoff, J. B.; Laurent, D.; Ly, H.; Stepp, J. *Chem. Eng. Technol.* **1998**, *21*, 757.
- (23) DeLongchamp, D.; Hammond, P. T. *Adv. Mater.* **2001**, *13*, 1455.
- (24) Liu, S. Q.; Kurth, D. G.; Mohwald, H.; Volkmer, D. *Adv. Mater.* **2002**, *14*, 225.
- (25) Cutler, C. A.; Bouguettaya, M.; Reynolds, J. R. *Adv. Mater.* **2002**, *14*, 684.
- (26) DeLongchamp, D. M.; Kastantin, M.; Hammond, P. T. *Chem. Mater.* **2003**, *15*, 1575.
- (27) DeLongchamp, D. M.; Hammond, P. T. In *Chromogenic Phenomena in Polymers*; Jenekhe, S. A., Kiserow, D. J., Eds.; ACS Symposium Series; American Chemical Society: Washington, DC, 2004.
- (28) DeLongchamp, D. M.; Hammond, P. T. *Adv. Funct. Mater.* **2004**, *14*, 224.

- (29) Jelle, B. P.; Hagen, G. *Sol. Energy Mater.* **1999**, *58*, 277.
- (30) Leventis, N.; Chung, Y. C. *J. Electrochem. Soc.* **1990**, *137*, 3321.
- (31) Jelle, B. P.; Hagen, G.; Birketveit, O. *J. Appl. Electrochem.* **1998**, *28*, 483.
- (32) Jelle, B. P.; Hagen, G. *J. Appl. Electrochem.* **1998**, *28*, 1061.
- (33) Duek, E. A. R.; Depaoli, M. A.; Mastragostino, M. *Adv. Mater.* **1992**, *4*, 287.
- (34) Duek, E. A. R.; Depaoli, M. A.; Mastragostino, M. *Adv. Mater.* **1993**, *5*, 650.
- (35) Jelle, B. P.; Hagen, G. *J. Appl. Electrochem.* **1998**, *28*, 1061.

Rubner and co-workers.<sup>36,37</sup> PANI was fully dissolved in dimethylacetamide (Aldrich); the resultant solution was then added to acidic (pH 3) Milli-Q (Millipore deionized, >18.2  $\Omega$  cm, 0.22  $\mu$ m filtered) water. After complete mixing, solutions were adjusted to pH 2.5 using HCl. PB dispersion synthesis was identical to that previously described.<sup>28</sup> ITO-glass substrates with dimensions 0.7 cm  $\times$  5 cm (Delta Technologies, 6  $\Omega$ /sq) were cleaned by ultrasonication in a series of solvents, dichloromethane, methanol, acetone, and Milli-Q water, for 15 min each, followed by a 5-min oxygen plasma etch (Harrick PCD 32G) to provide a clean, hydroxyl-rich surface. Substrates were used immediately following cleaning.

**Assembly.** Film assembly was automated with a Carl Zeiss HMS DS-50 slide stainer. The substrates were exposed to PANI solution for 10 min, followed by copious water rinsing for 4 min in three consecutive baths containing the Milli-Q water/dimethylacetamide solvent pair at pH 2.5. The substrates were then placed in a custom-built ultrasonic cleaner (Advanced Sonic Processing) containing pH 2.5 Milli-Q water for 4 min. Finally, substrates were exposed to the PB dispersion for 10 min and again rinsed for 4 min in three consecutive Milli-Q water baths at pH 2.5. This cycle was repeated for the required number of layer pairs.

**Characterization.** Thickness and roughness measurements were performed on the constructed films with a Tencor P10 profilometer using a 2  $\mu$ m stylus tip and 5 mg stylus force; profiling was performed by scoring a portion of the film down to the substrate and then profiling the score. Film thickness was measured by a Gaertner single-wavelength ellipsometer atop silicon substrates for films of thickness less than 500 Å, using a fixed incident angle of 70°. Roughness for these thinner films was evaluated using profilometry. Electrochemical potential control and current sensing were performed using an EG&G 263A potentiostat/galvanostat. The electrolyte was 0.1 M H<sub>2</sub>SO<sub>4</sub> + 0.1 M KCl, the counter electrode was 4 cm<sup>2</sup> platinum foil, and reference electrode was K-SCE. Cyclic voltammetry was performed by cycling between 0.6 and -0.2 V at 0.025, 0.05, 0.1, 0.2, and 0.4 V/s. Potential step chronoamperometry was performed by stepping between -0.2 and 0.6 V vs K-SCE, with 30 s per step and 60 s per cycle. For all films, 20 cycles were performed sequentially before the measurement cycle. For spectroelectrochemistry, films assembled atop ITO were positioned in a quartz cell with electrolyte, platinum counter electrode, and K-SCE. Spectral characterization was performed with a StellarNet EPP2000 concave grating UV-vis-NIR spectrophotometer with combined incandescent and deuterium lamp sources.

## Results and Discussion

**Assembly.** The PB nanoparticle suspension was synthesized as we have described previously.<sup>28</sup> To summarize, the suspension consists of polydisperse pure PB particles in the range of 1–10 nm, with a PB unit cell concentration in the dispersion of 0.010 M. The particles are “soluble” PB, possessing an anionic surface with dissociable potassium cations. PANI solutions were prepared with a dimethylacetamide/water solvent pair as has been described by Rubner and co-workers.<sup>36,37</sup> The PB dispersion and PANI solution were adjusted to pH 2.5. The assembly of PANI/PB nanocomposite films proceeded with the automated exposure of clean indium-tin oxide-coated glass (ITO) to (1) PANI solution for 10 min, (2) a 4-min solvent pair rinse at pH 2.5, (3) an ultrasonically agitated pH 2.5 water rinse for 4 min, (4) the aqueous PB dispersion for 10 min, and (5) a 4-min water rinse at pH 2.5. These five steps were then repeated for the required number of layer pairs. The

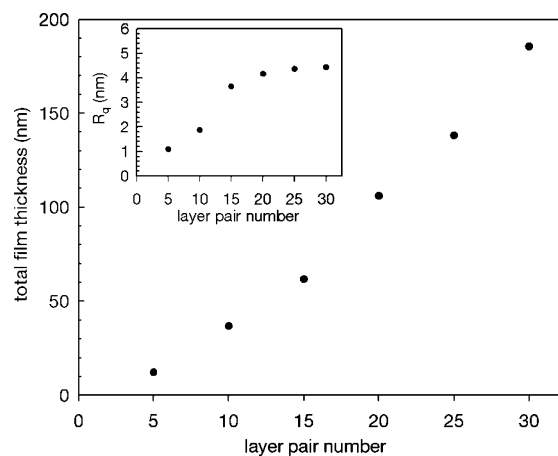


**Figure 1.** Correlation of film thickness to layer pair number for the PANI/PB series. The root-mean-square roughness is shown in the inset.

system pH was maintained at pH 2.5 throughout assembly; this provision enhanced the assembled film smoothness and uniformity by ensuring that PANI retained a net positive ionization. No destabilization of the PB dispersion was observed at pH 2.5. Subjecting the films to ultrasonic agitation further enhanced smoothness; this step was found to reduce film roughness by at least 50%. Ultrasonic agitation has proved successful at discouraging nonspecific adsorption during the selective deposition of LBL-assembled systems upon micropatterned, chemically templated surfaces.<sup>38,39</sup> During assembly of PANI/PB we believe that film smoothness is enhanced by the ultrasonic removal of poorly bound or agglomerated PB to achieve a near-monolayer of adsorbed particles.

The LBL growth of PANI/PB films under these conditions is classically linear, as shown in Figure 1. The PANI/PB films increase in thickness by 6.9 nm per layer pair, which is thicker than the 4.1 nm per layer pair of the LPEI/PB series,<sup>28</sup> mostly likely due to the lower ionization density of PANI polycation chains as compared to LPEI chains. The roughness of this series is slightly higher than that of LPEI/PB most likely for the same reason. It should be noted that the roughness of PANI/PB remains less than or equal to the ~4 nm average PB particle size. Linear growth indicates the successful combination of PANI and PB without complications that have arisen from superlinear growth in other LBL-assembled systems containing two electroactive species.<sup>26</sup> It should also be noted that LBL-assembled PANI/PB films exhibit far superior smoothness and substrate adhesion than do electrochemically deposited PANI + PB electrode films, which commonly suffer from high roughness visible to the naked eye and flaking delamination.<sup>35</sup>

**Electrochemistry.** Cyclic voltammetry was employed to investigate the PANI/PB system over a potential range from -0.2 to 0.6 V vs K-type SCE. Cycling to potentials more anodic than 0.6 V in order to access the second oxidation of PANI to nigraniline inevitably causes PANI degradation due to hydrolysis of the imine group and subsequent chain scission.<sup>40–42</sup> More anodic potentials also lead to the second oxidation

(36) Cheung, J. H.; Stockton, W. B.; Rubner, M. F. *Macromolecules* **1997**, *30*, 2712.

(37) Stockton, W. B.; Rubner, M. F. *Macromolecules* **1997**, *30*, 2717.

(38) Clark, S. L.; Hammond, P. T. *Adv. Mater.* **1998**, *10*, 1515.

(39) Clark, S. L.; Hammond, P. T. *Langmuir* **2000**, *16*, 10206.



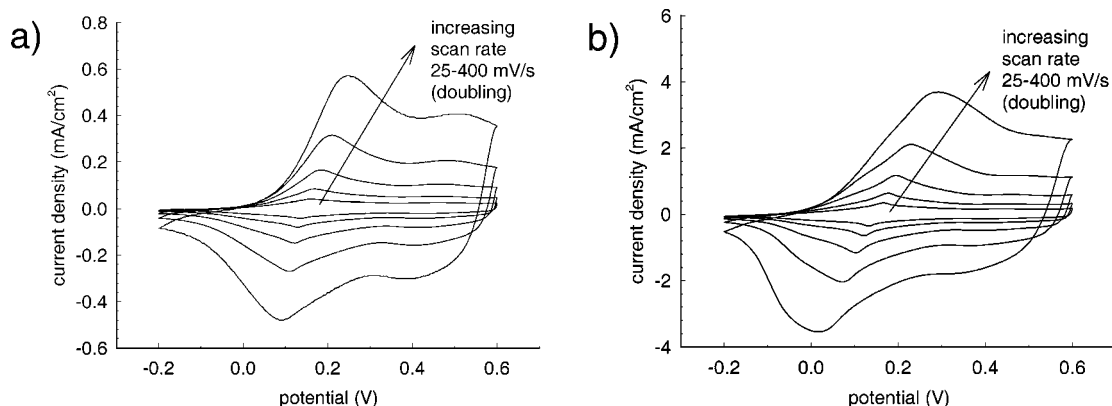


**Figure 2.** Cyclic voltammetry of PANI/PB: (a) 5 layer pairs and (b) 20 layer pairs. The arrow indicates increasing scan rate, which doubles (e.g. 25, 50, 100, 200, 400 mV/s) for each sequential curve. Electrolyte was 0.1 M sulfuric acid + 0.1 M potassium chloride and potentials are reported vs a K-type saturated calomel reference.

of PB particles to the Prussian brown state. This state possesses no ionization, a condition that eventually causes film dissolution due to the resulting electrostatic self-repulsion of the polycation,<sup>28</sup> which in this case is not desired. Cyclic voltammograms of some films of the PANI/PB series are shown in Figure 2. The single broad wave corresponds to two overlapped transitions: (1) PANI transforms reversibly between reduced leucoemeraldine and oxidized emeraldine salt and (2) PB transforms from the reduced  $K_2Fe^{II}[Fe^{II}(CN)_6]$  (PW) to the oxidized  $KFe^{III}[Fe^{II}(CN)_6]$  (PB). Note that potassium cations are shown in PB chemical formulas for clarity; we expect substitution of PANI cationic sites for surface potassium cations in fully assembled films. The PANI/PB half-wave potential  $E_{1/2}$  appears at approximately 0.11–0.15 V vs K-SCE, which corresponds well to those observed in LBL films containing PANI and PB separately combined with electrochemically inert polymers.<sup>23,27,28</sup>

In general, there exists an increasing resistance to reduction and oxidation with increasing film thickness, as is typically observed for organic redox-active electrode films. This increasing resistance is revealed in Figure 2 by an increasing hysteresis between oxidative and reductive current waves as scan rates increase. In general, however, linearity is maintained between scan rates and peak heights, indicating that the reaction is not limited by ionic diffusion into the electrode film, but rather is rate-controlled by internal resistance within the layers. As would be expected, the resistance observed in the PANI/PB composite is far less than that observed previously in LPEI/PB;<sup>28</sup> the PANI within the matrix appears to greatly facilitate the conduction of electrons throughout the film.

Although not immediately discernible from Figure 2, contributions from both PANI and PB electrochemistry can be ascertained from cyclic voltammetry. The electrochemistry for both materials occurs over very similar potential ranges so that the waves are almost exactly superimposed. It is possible to distinguish individual contributions of PANI and PB at slow scan rates; a comparison is offered in Figure 3. This figure compares

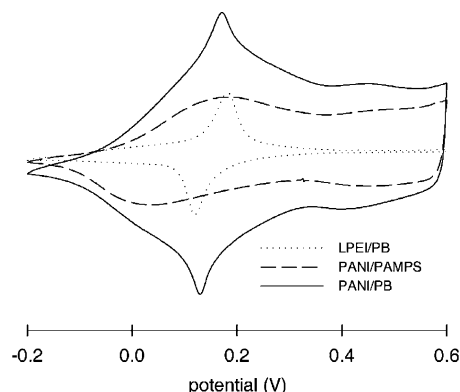


**Figure 3.** Comparison of cyclic voltammetry of several LBL composites: the LPEI/PB composite exhibits only PB electrochemistry, the PANI/poly(2-acrylamido-2-methyl-1-propanesulfonic acid) (PANI/PAMPS) composite exhibits only PANI electrochemistry, and the PANI/PB composite exhibits both. Scans shown were at a rate of 25 mV/s, and all potentials are vs K-SCE; the vertical axis is scaled current.

cyclic voltammetry scans of the 30 layer pair PANI/PB composite, a 15 layer pair PANI/poly(2-acrylamido-2-methyl-1-propanesulfonic acid) (PANI/PAMPS) composite, and a 20 layer pair LPEI/PB composite. Individual contributions of PANI and PB within the PANI/PB composite are clearly visible, as the nature of the two redox peaks is different. The PANI contributes broad reduction and oxidation peaks, with sloping shoulders, while PB contributes sharper, better defined peaks. In the scan of the PANI/PB composite, the sloping broad peaks of PANI dominate the cyclic voltammogram *except* at the expected potentials of PB electrochemistry where the PB peaks “emerge” from the broader PANI electrochemistry. Cyclic voltammograms of the PANI/PB nanocomposite are consistent with those reported from earlier studies of combined PANI + PB electrochemistry,<sup>30</sup> though in this case the deconvolution of individual contributions is more straightforward. This comparison illustrates definitively that both materials are electrochemically functional within the LBL assembled film, exhibiting explicit electrochemical signatures.

Square wave switching was next applied to the PANI/PB composites to determine whether PANI and PB are completely electrochemically accessible, even in very thick films. Results of switching are shown in Figure 4. As expected, switching speed decreases with increasing

(40) Kobayashi, T.; Yoneyama, H.; Tamura, H. *J. Electroanal. Chem.* **1984**, *161*, 419.

(41) Huang, W. S.; Humphrey, B. D.; MacDiarmid, A. G. *J. Chem. Soc.-Faraday Trans.* **1986**, *82*, 2385.

(42) Huang, W. S.; MacDiarmid, A. G. *Polymer* **1993**, *34*, 1833.

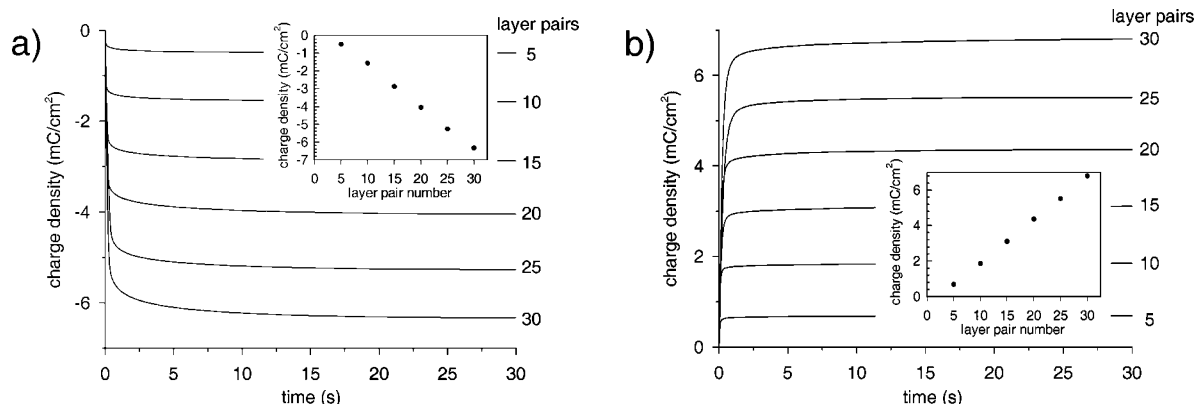


**Figure 4.** Square wave switching of the PANI/PB series: Faradaic charge response to (a) oxidation from  $-0.2$  to  $0.6$  V and (b) reduction from  $0.6$  to  $-0.2$  V. Insets indicate the limiting (30 s) charge density vs layer pair number. Electrolyte was  $0.1$  M sulfuric acid +  $0.1$  M potassium chloride and potentials are reported vs a K-type saturated calomel reference.

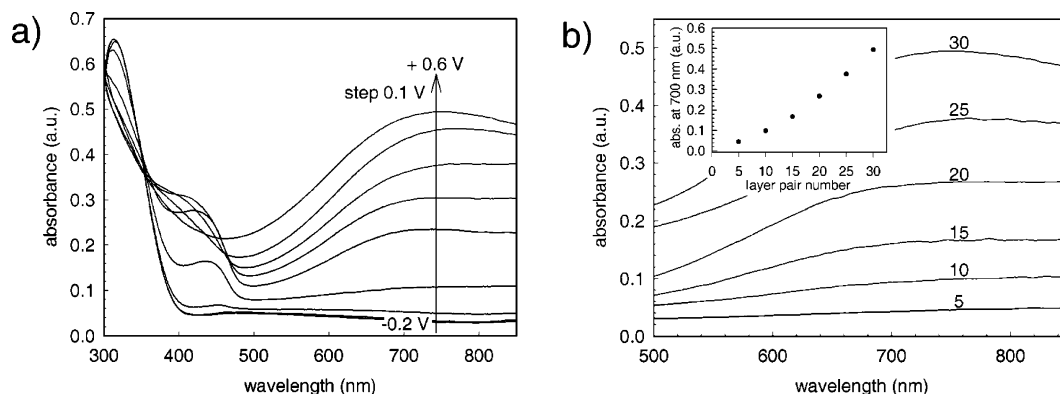


**Figure 5.** Spectroelectrochemistry of the PANI/PB series: (a) absorbance of a 30 layer pair PANI/PB nanocomposite increases as potential becomes more anodic; oxidation proceeds from  $-0.2$  V to  $0.6$  V in a stepwise fashion with a step size of  $0.1$  V. Spectra shown are postequilibration at each potential. (b) Absorbance at  $0.6$  V as a function of layer pair number.

film thickness, with an observably slower asymptotic approach to the limiting Faradaic charge density. As can be seen in the Figure 4 inset, this maximum Faradaic charge density increased linearly with increasing film thickness, indicating that the PANI and PB within the films remain fully electrochemically accessible within the nanocomposite, regardless of film thickness or layer pair number. This result of full electrochemical accessibility reveals a film in which charge percolation is possible throughout the film thickness, due either to direct electron conduction or redox exchanges. Electrochemical changes are not partial or localized near the electrode surface but rather are complete and distributed throughout the entire film. This observation is critical, as it confirms that this LBL assembly strategy allows the construction and tuning of thin films in which all elements within the film are accessible and functional. Film thickness can be optimized to enhance contrast, and inserted layers of varying composition will be accessed.

**Spectroelectrochemistry.** In Figure 5, we present the spectroelectrochemistry of the PANI/PB nanocomposite series. The spectroelectrochemistry reveals complete conversion from a pale yellow, transmissive state to a highly colored blue state with a peak absorbance at approximately  $750$  nm. The lack of absorbance at cathodic potentials confirms the absence of electrochemically inaccessible PANI or PB. The oxidized state features a very broadband absorbance that increases linearly with film thickness, with no profound shifts in

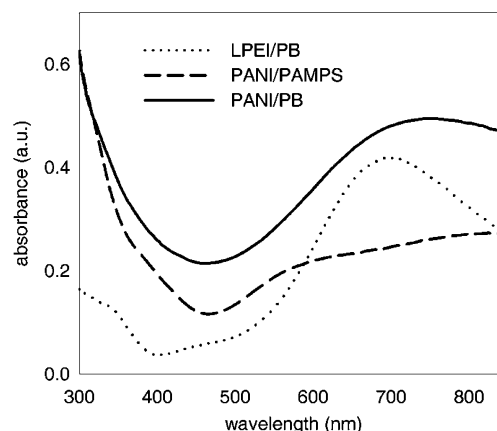


**Figure 6.** Comparison of fully oxidized ( $0.6$  V vs K-SCE) absorbance spectra of an LPEI/PB composite, a PANI/PAMPS composite, and the PANI/PB composite.

peak location or spectral character. At an intermediate potential of  $0.2$  V, the spectrum in Figure 5a exhibits absorbance at  $400$ – $450$  nm and broad absorbance at  $600$ – $800$  nm; the combination should result in a green hue.

Individual contributions to the absorbance character of these dual electrochrome films can be distinguished from the UV–vis absorbance spectra of the films in the fully colored, oxidized state. Figure 6 offers a comparison of the PANI/PB absorbance spectrum with spectra of two other LBL-assembled films representative of PANI and PB individually. The coloration of PANI/PB is

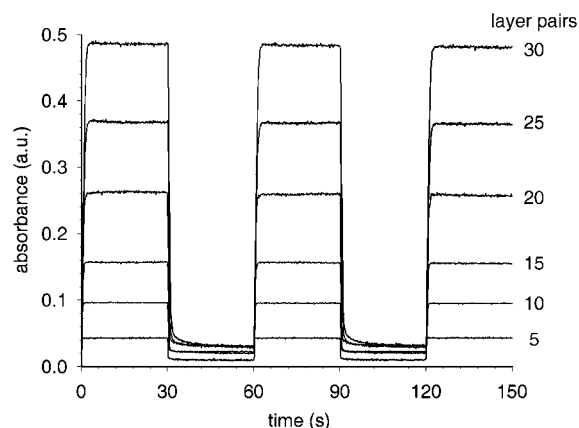


**Figure 7.** The absorbance response at 750 nm of PANI/PB films subjected to a square-wave switching potential. Switching occurred between  $-0.2$  V (low absorbance) and  $0.6$  V (high absorbance) for 30 s at each potential.

clearly the result of the addition of the two chromophores. The characteristic absorbance of PANI at 300 nm is reproduced in the PANI/PB composite, as is the PB peak at 700–800 nm. The PB peak location is red-shifted in the PANI/PB composite due to the addition of the PANI shoulder from 600 to 800 nm. The PB enhances the red absorbance, resulting in a darker and truer blue than the usual blue/green of oxidized PANI.

Because the strong absorbance at 600–800 nm is the sum of PANI and PB coloration, the contributions of each can be determined. From the concentration of redox centers based on the Faradaic charge uptake of PANI/PB, the extinction coefficient for the oxidized state of this system is  $7040 \text{ M}^{-1} \text{ cm}^{-1}$  at 750 nm and  $6690 \text{ M}^{-1} \text{ cm}^{-1}$  at 700 nm. From our previous PANI work, a counterpolymer-dependent extinction coefficient of  $4260\text{--}5570 \text{ M}^{-1} \text{ cm}^{-1}$  at 700 nm was found, with an average of  $\sim 4950 \text{ M}^{-1} \text{ cm}^{-1}$ .<sup>27</sup> The LPEI/PB system exhibited an extinction coefficient of  $8020 \text{ M}^{-1} \text{ cm}^{-1}$  at 700 nm. On the basis of these figures, and assuming that the extinction values of PB and PANI are not significantly altered, the relative coloration contribution of PANI to PB is 0.43:0.57. Each PB chromophore is well-defined as a single unit cell of a PB nanocrystal, but the chromophore definition is less precise in the case of the PANI conducting polymer, where one effective chromophore might be distributed over several repeats. A full composition profile thus cannot be determined without additional information concerning the extent of oxidation or reduction of PANI.

**Optical Switching.** The optical switching of the PANI/PB series can be measured at the peak wavelength of 750 nm with results as shown in Figure 7. On the basis of the sharp appearance of the spectral response to a square-wave potential, it is apparent that the PANI/PB series switches color extremely fast. Quantification of switching times can be made by defining a change in 90% of the total absorbance span as indicating switching completion. A tabulation of the switching times based on this criterion is shown in Table 1. With switching time consistently lower than 1.5 s, these films switch faster than any other LBL-assembled electrochromic films with a similar caliber of contrast. PANI/PB switches far faster than previously reported devices incorporating electrochemically deposited PANI and PB electrodes, which switch in 3–120 s.

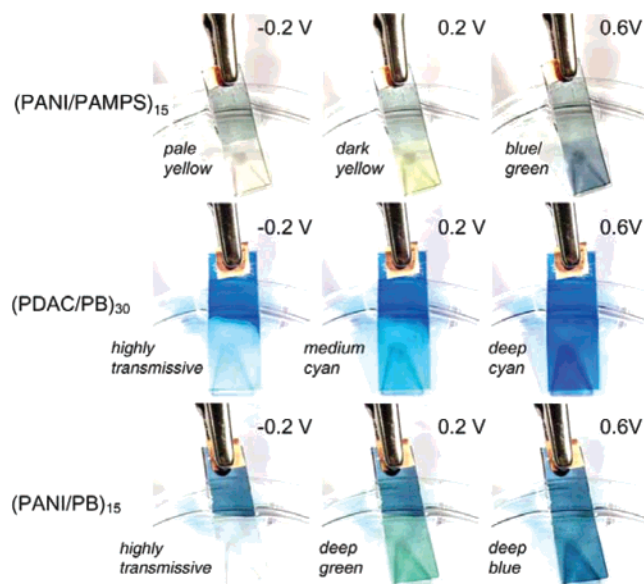


**Figure 8.** Photographs of the electrochromism of PANI/PB and the origins of multiple color electrochromism in this dual electrochrome composite. Films were photographed immersed in an electrochemical cell; the electrolyte meniscus is visible on the upper portion of the film. Photographs were collected after a 30-s equilibration at the noted potential. These particular films were created using a spin-coating variant of LBL assembly.<sup>43</sup> For PB-only electrochromism, an LBL-assembled film containing the colorless and electrochemically inert polycation poly(diallyldimethylammonium chloride) (PDAC) is included here for variety; multiple images of LPEI/PB films are available in our prior publication.<sup>28</sup>

**Table 1. Switching Time and Contrast of the PANI/PB Series**

layer pairs	color time (s)	bleach time (s)	$\Delta\%T$ ( $\lambda = 750 \text{ nm}$ )
5	0.31	0.49	8.2
10	0.66	0.66	15.4
15	0.90	0.66	26.4
20	1.15	0.85	39.7
25	1.58	1.28	55.5
30	1.62	1.52	61.1

The coloration of PANI/PB is demonstrated in Figure 8, along with the coloration of PANI and PB single-electrochrome composites. The origins of multiple hue electrochromism are apparent on examination of these photographs. In the reduced state, both PANI and PB are almost colorless, resulting in a highly transmissive appearance. At an intermediate potential of 0.2 V, PANI displays a dark yellow color. The PB composite displays a pale blue color at this intermediate potential because not all of the PB within the film is oxidized. The combination of intermediate colors results in an intermediate color of almost pure green for the PANI/PB composite. Finally, upon full oxidation, the PANI/PB film achieves a dark navy blue color. The authors note that yellow to green to blue color transitions have been achieved in specially synthesized conducting polymers, in particular those based on a bis(ethylenedioxythiophene)-N-substituted carbazole motif.<sup>15</sup> The PANI/PB composite provides an alternative of greater synthetic simplicity that possesses a more transmissive bleached state. The LBL assembly additive electrochromism strategy could incorporate a variety of specially synthesized conducting polymers (which can be made into polyelec-

trolytes)<sup>25</sup> to cover an even wider portion of the CMYK color space. Innovative synthesis and assembly-based processing will work together to promote the development of electrochromic devices into ubiquitous, full-color displays.

### Conclusions

A multiple-hue dual electrochrome composite has been developed on the basis of the LBL assembly of two anodically electrochromic materials—PANI, a conjugated polymer that colors based on the oxidative creation of electronically conducting polaronic states, and an inorganic nanoparticle dispersion of PB that colors based on the oxidative alteration of a charge-transfer pair from  $\text{Fe}^{\text{II}}\text{—Fe}^{\text{II}}$  to  $\text{Fe}^{\text{II}}\text{—Fe}^{\text{III}}$ . The PANI/PB series grows linearly in thickness with layer pair number, providing extremely smooth films with roughness no greater than 4 nm.

As the PANI/PB nanocomposite increases in thickness, both PANI and PB within the layers remain completely electrochemically accessible, as indicated by a linear increase in the Faradaic charge capacity with increasing layer thickness. Discrete signatures of both materials are visible in cyclic voltammetry scans, and spectrophotometry also confirms distinct absorbance contributions from both components. The extinction coefficient of this system was found to be between those of PANI and PB; a chromophore ratio of PANI:PB was calculated to be 0.77. With information describing the extent of PANI oxidation, an exact composition profile could be calculated from this quantity.

The PANI/PB system was engineered with the expectation of multiple hues due to the different coloration gray scale responses of PANI and PB. This expectation was substantiated; the color of PANI/PB films changes from a highly transmissive reduced state to an intermediate partially oxidized green color to a navy blue fully oxidized color. This result confirms the validity of this strategy for the design of multiple-hue electrochromic electrode films; the technique can be extended to

even more useful colors, initially taking advantage of the wide color spectrum of hexacyanoferrate nanoparticle suspensions, and perhaps later extending to differently colored states based on poly(viologens) or water-soluble conjugated polymer systems.<sup>25</sup> Aside from displaying multiple hues, PANI/PB performed well as an electrochromic material. Color change response times were fast; the presence of conducting PANI enhances electron transport and thus significantly increases switching speed. High contrast was also achieved due to the high density of electrochromic material within the electrode films and the substantial extinction of each chromophore.

The LBL assembly technique provides almost limitless possibilities for the combination of electrochromic species into intelligently designed composites that can meet a host of applications. These systems will utilize simple, low cost polymers that are commercially available and inorganic nanoparticles that are readily and cheaply synthesized. These materials will be assembled into composite films that can be made exceedingly thin and will be easily micropatterned,<sup>38,39,44,45</sup> making them ideal for electronic paper and lightweight display applications. Extension to other fields may follow, and this technology may impact bio- and electrocatalysis, magnetic storage, and sensing.

**Acknowledgment.** Special appreciation is extended to Prof. Kookheon Char of Seoul National University for gracious assistance with spin LBL assembly. The authors thank the DOD NDSEG program and the ARO TOPS MURI for support. This work was also supported by the MIT MRSEC Program of the National Science Foundation under award DMR 94-00334.

CM0496624

(43) Cho, J.; Char, K.; Hong, J.-D.; Lee, K.-B. *Adv. Mater.* **2001**, *13*, 1076.

(44) Hammond, P. T.; Whitesides, G. M. *Macromolecules* **1995**, *28*, 7569.

(45) Jiang, X. P.; Zheng, H. P.; Gourdin, S.; Hammond, P. T. *Langmuir* **2002**, *18*, 2607.